Title

Synapses are regulated by the cytoplasmic tyrosine kinase Fer in a pathway mediated by p120catenin, Fer, SHP-2, and beta-catenin.

Journal

The Journal of cell biology, 183(5)

ISSN

0021-9525

Authors

Lee, Seung-Hye
Peng, I-Feng
Ng, Yu Gie
et al.

Publication Date

2008-12-01

DOI

10.1083/jcb.200807188

Peer reviewed

Synapses are regulated by the cytoplasmic tyrosine kinase Fer in a pathway mediated by p120catenin, Fer, SHP-2, and β-catenin

Seung-Hye Lee,[1] I.-Feng Peng,[2] Yu Gie Ng,[1] Masahiro Yanagisawa,[4] Shernaz X. Bamji,[1] Lisa P. Elia,[1] Janne Balsamo,[5] Jack Lilien,[5] Panos Z. Anastasiadis,[4] Erik M. Ullian,[1,2,3] and Louis F. Reichardt[1,3]

[1]Department of Physiology, [2]Department of Ophthalmology, and [3]Neuroscience Program, University of California, San Francisco, San Francisco, CA 94158
[4]Cell Adhesion and Metastasis, Department of Cancer Biology, Mayo Clinic, Jacksonville, FL 32224
[5]Department of Biological Sciences, University of Iowa, Iowa City, IA 52242

Localization of presynaptic components to synaptic sites is critical for hippocampal synapse formation. Cell adhesion–regulated signaling is important for synaptic development and function, but little is known about differentiation of the presynaptic compartment. In this study, we describe a pathway that promotes presynaptic development involving p120catenin (p120ctn), the cytoplasmic tyrosine kinase Fer, the protein phosphatase SHP-2, and β-catenin. Presynaptic Fer depletion prevents localization of active zone constituents and synaptic vesicles and inhibits excitatory synapse formation and synaptic transmission. Depletion of p120ctn or SHP-2 similarly disrupts synaptic vesicle localization with active SHP-2, restoring synapse formation in the absence of Fer. Fer or SHP-2 depletion results in elevated tyrosine phosphorylation of β-catenin. β-Catenin overexpression restores normal synaptic vesicle localization in the absence of Fer or SHP-2. Our results indicate that a presynaptic signaling pathway through p120ctn, Fer, SHP-2, and β-catenin promotes excitatory synapse development and function.

Introduction

Chemical synapses are specialized asymmetric cellular interaction sites designed for efficient information transmission (Yamada and Nelson, 2007). Synapse formation is a tightly regulated multistep process involving reciprocal interactions between presynaptic and postsynaptic cells (Goda and Davis, 2003; McAllister, 2007). Presynaptic assembly requires targeted delivery of constituents of the synaptic plasma membrane, such as calcium channels and target SNARES, synaptic cytomatrix constituents, such as Bassoon and Piccolo, and synaptic vesicles (Ahmari et al., 2000; Dresbach et al., 2003; Krueger et al., 2003). Synaptic vesicles are docked and released preferentially in a morphologically distinct domain of the nerve terminal named the active zone, which is formed by fusion to the plasmalemma of active zone precursor vesicles called Piccolo–Bassoon transport vesicles (Dresbach et al., 2006). Signals from the presynaptic axon promote differentiation of specialized zones on the postsynaptic side of the synapse that include transmitter receptors, scaffold proteins, cytoskeletal constituents, and signaling molecules, whereas reciprocal signals from the postsynaptic cell induce further maturation of the presynaptic nerve terminal. In the mammalian central nervous system, excitatory synapses are formed primarily on dendritic spines, actin-rich structures that concentrate the molecules required for postsynaptic signaling (Tada and Sheng, 2006; McAllister, 2007).

Compared with the extensive studies on mechanisms that control spine morphogenesis and postsynaptic protein localization (Tada and Sheng, 2006; Alvarez and Sabatini, 2007; Bourne and Harris, 2008), our understanding of presynaptic development is limited. A recent RNAi screen for decreased acetylcholine secretion in *Caenorhabditis elegans* identified several genes

Correspondence to Seung-Hye Lee: Seung-Hye.Lee@ucsf.edu; or Louis F. Reichardt: Louis.Reichardt@ucsf.edu

S.X. Bamji's present address is Dept. of Cellular and Physiological Sciences, University of British Columbia, Vancouver, British Columbia V6T 1Z3, Canada.

L.P. Elia's present address is Elan Pharmaceuticals, Inc., South San Francisco, CA 94080.

Abbreviations used in this paper: CAZ, cytomatrix of active zone; DIV, day in vitro; EPSC, excitatory postsynaptic current; eEPSC, evoked EPSC; IP, immunoprecipitation; p120ctn, p120catenin; shRNA, small hairpin RNA; WT, wild type.

The online version of this article contains supplemental material.

The Rockefeller University Press $30.00
J. Cell Biol. Vol. 183 No. 5 893–908
www.jcb.org/cgi/doi/10.1083/jcb.200807188

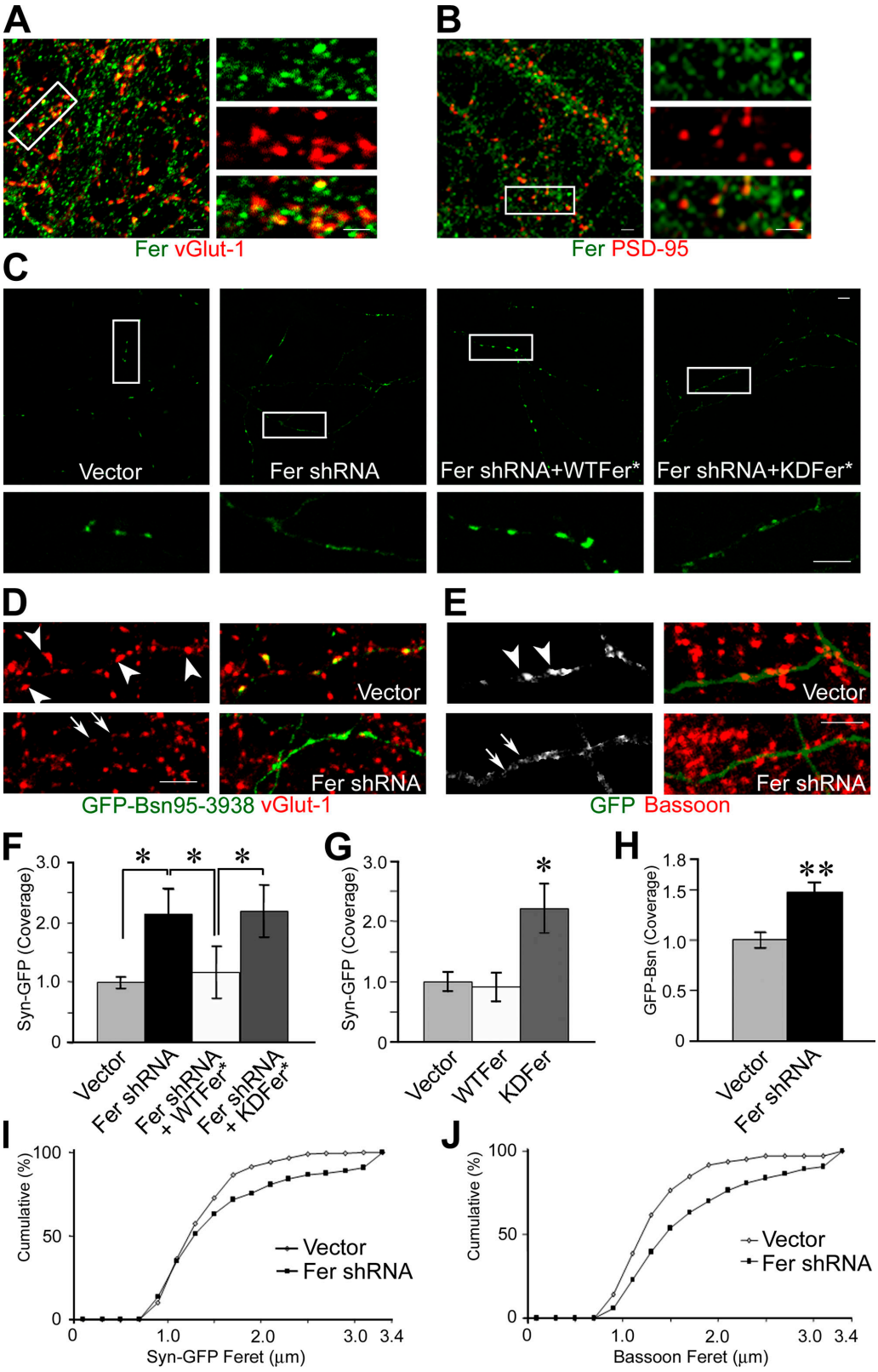

Figure 1. **Localization of Fer at excitatory synapses and delocalization of synaptic vesicle and CAZ puncta after knockdown of Fer.** (A and B) 14 DIV dissociated rat hippocampal neurons were stained with anti-Fer and anti-vGlut1 (A) or anti–PSD-95 (B) antibodies. (C) Localization of synaptophysin-GFP in 14 DIV hippocampal neurons that were transfected at 10 DIV with synaptophysin-GFP together with the indicated constructs. (D) Localization of GFP–Bsn95-3938 in 14 DIV hippocampal neurons transfected at 10 DIV with GFP–Bsn95-3938 plus control or Fer shRNA vector. Cultures were stained with anti-vGlut1 antibody. (E) 10 DIV neurons were transfected with GFP-containing vector or Fer shRNA and stained with Bassoon antibody. (left) Images were processed to indicate that Bassoon colocalized with GFP. (F and G) The coverage (normalized micrometers of GFP per 10 μm of axon length; see Materials and methods) of synaptophysin-GFP (Syn-GFP) puncta along axons in each indicated condition. In F, $n = 7$ (vector), 11 (Fer shRNA), 15 (Fer shRNA + WTFer*), and

that had not previously been implicated in synapse transmission, including Fer tyrosine kinase (Sieburth et al., 2005).

The mechanisms by which Fer might regulate synapse structure and function have not been studied. Fer has been shown to act in several signaling pathways, including receptor tyrosine kinase and cell adhesion molecule–regulated signaling. Recent work using chick retinal neuroepithelial cells has indicated that Fer promotes the integrity of the cadherin complex through phosphorylation of a tyrosine phosphatase PTP1B, which promotes dephosphorylation of β-catenin Y654, thereby promoting cadherin–β-catenin interactions (Xu et al., 2004). In contrast, a separate study showed that Fer increased the phosphorylation of β-catenin Y142, which inhibited the interaction between β-catenin and α-catenin (Piedra et al., 2003). In this study, we identify an intracellular signaling pathway mediated by p120catenin (p120ctn), Fer, and the protein tyrosine phosphatase SHP-2 that regulates β-catenin phosphorylation and promotes presynaptic differentiation through localization of synaptic vesicles and the active zone–associated protein Bassoon.

Results

Cell-autonomous ablation of Fer function results in dispersion of synaptic vesicle puncta and cytomatrix of active zone (CAZ) puncta along the axon

In the mouse hippocampus, Fer is widely expressed, including in CA1 and CA3 neurons (Fig. S1 A, available at http://www.jcb.org/cgi/content/full/jcb.200807188/DC1). In cultured hippocampal neurons, Fer is present in punctate structures along both dendrites and axons (Fig. S1 B). A subset of the Fer-labeled puncta is associated with vGlut1 and PSD-95, markers of the presynaptic and postsynaptic compartments of excitatory synapses, respectively (Fig. 1, A and B). We verified that the observed colocalization is significant by comparing the images with mismatched images created by shifting of one channel along the x axis relative to other channels of the original images (Fig. S1, C and D).

To determine whether Fer regulates synaptic development, we used plasmid-based expression of small hairpin RNAs (shRNAs) in cultured hippocampal neurons (Fig. S2, available at http://www.jcb.org/cgi/content/full/jcb.200807188/DC1). To examine presynaptic development, an expression vector encoding the synaptic vesicle marker synaptophysin-GFP was cotransfected with Fer shRNA (Fig. 1 C). Fluorescence-tagged synaptic vesicle marker proteins have been widely used to visualize presynaptic sites (Ahmari et al., 2000; Ryan and Reuter, 2001; Lim et al., 2008). Along control neuron axons, synaptophysin-GFP exhibited rounded or slightly elongated ∼1-µm-long clusters plus smaller and less intense clusters, which is consistent with prior studies (Nakata et al., 1998; Antonova et al., 2001). In contrast, in the Fer shRNA–expressing neurons the synaptophysin-GFP puncta were less well focused and more diffuse. Coexpression of shRNA-resistant Fer restored the normal pattern of synaptic vesicle localization. Coexpression of an shRNA-resistant kinase-dead Fer mutant, however, failed to rescue the presynaptic phenotype, indicating that the kinase activity of Fer is necessary for normal presynaptic development (Fig. 1 C). Overexpression of kinase-dead Fer also resulted in synaptophysin-GFP diffusion (Fig. S3). To quantitate the effect of shRNA knockdown on presynaptic terminals, we measured the coverage of synaptophysin-GFP puncta along transfected axons at low threshold brightness. The coverage of synaptophysin-GFP along axons was significantly increased in Fer shRNA– or kinase-inactive Fer-transfected axons compared with controls (Fig. 1, F and G). In addition, individual synaptophysin-GFP puncta exhibited increased length and decreased intensity in Fer-deficient neurons (Fig. 1 I and see Fig. 3 J). We confirmed that the knockdown of Fer had similar effects on endogenous proteins as well by immunostaining with antibodies to the excitatory presynaptic marker vGlut1, which exhibited diffused weak intensity localization in Fer-deficient axons (Fig. 1 D, arrows) in contrast to concentrated puncta in controls (Fig. 1 D, arrowheads). Overexpression of wild-type (WT) Fer in control neurons did not result in significant changes in the intensity or size of synaptophysin-GFP puncta (unpublished data).

We next examined the localization of a protein associated with CAZ using a GFP-tagged Bassoon variant (GFP–Bsn95-3938) that has been used to identify the CAZ in neurons (Dresbach et al., 2003; Bresler et al., 2004). GFP-Bassoon colocalized with vGlut1 immunoreactive puncta in control neurons, but in Fer-deficient cells GFP-Bassoon puncta were dispersed along the axons (Fig. 1 D). We observed this weakening of Bassoon puncta when we checked endogenous Bassoon by immunostaining along the Fer shRNA–transfected axons (Fig. 1 E). The coverage of GFP–Bsn95-3938 puncta was significantly increased in Fer-deficient axons compared with that of controls (Fig. 1 H). The individual Bassoon puncta were more diffuse in Fer-deficient axons compared with control axons (Fig. 1 J). Together, these results indicate that Fer is required for normal localization to synapses of both CAZ constituents and synaptic vesicles.

Knockdown of Fer increases the motility of presynaptic clusters

Next, we asked whether the absence of Fer affects the stability of synaptic vesicle clusters. Time-lapse studies have identified two classes of synaptic vesicle–associated clusters that can be distinguished by size and mobility: large clusters with relatively low mobility localized at synaptic sites and smaller and more mobile clusters believed to constitute a population of transport vesicles with directed and saltatory movements (Ahmari et al., 2000;

13 (Fer shRNA + kinase-dead mutant [K591R] of Fer [KDFer*]). In G, *n* = 10 (vector), 9 (WT Fer), and 9 (kinase-dead mutant [K591R] of Fer). (H) The axonal coverage of GFP–Bsn-95-3938. *n* = 12 (vector) and 13 (Fer shRNA). (I and J) The cumulative percentage curves representing the feret length of synaptophysin-GFP (I) and endogenous Bassoon (J). In I, *n* = 281 (vector) and 297 (Fer shRNA). In J, *n* = 425 (vector) and 572 (Fer shRNA). WTFer* and KDFer* are shRNA refractory constructs. Boxed areas in A–C are shown in high resolution images at the right (A and B) or bottom (C) of each panel. Arrows and arrowheads indicate vGlut1 or Bassoon immunoreactivity along the transfected axons. *, P < 0.05; **, P < 0.01. Error bars represent SEM. Bars, 5 µm.

Krueger et al., 2003; McAllister, 2007). In control axons, synaptophysin-GFP labeled both large puncta (~1 µm in major axis length) moving slowly or remaining stable (at 0.031 µm/min on average; Fig. 2 and Video 1, available at http://www.jcb.org/cgi/content/full/jcb.200807188/DC1) and smaller puncta (<0.4 µm in major axis length) moving much faster in the control. In contrast, in neurons expressing Fer shRNA, large puncta were highly mobile along the axons (at 0.276 µm/min on average; Fig. 2 and Videos 2 and 3). These puncta displayed variable velocities and irregular and undirected movement, indicating that these were not transport vesicles (McAllister, 2007). These results indicate that loss of Fer reduces the efficiency with which synaptic vesicle clusters are localized at synaptic sites.

Presynaptic Fer is required for proper excitatory synapse formation and dendritic spine morphogenesis

Next, we asked whether the presynaptic Fer knockdown–mediated destabilization of presynaptic compartments affects the formation of excitatory synapses. Compared with controls, knockdown of Fer resulted in a significant reduction in the colocalization of synaptophysin-GFP puncta with the excitatory postsynaptic marker PSD-95 (Fig. 3, A and B). Overexpression of kinase-dead Fer in neurons had a similar effect, indicating that Fer kinase activity is necessary in regulating excitatory synapse formation (Fig. S3).

Maturation of dendritic spines requires interactions between the pre- and postsynaptic compartments (Okabe et al., 2001; Bourne and Harris, 2008). To determine whether spine morphogenesis is also affected by presynaptic Fer knockdown, we used electroporation to label WT neurons with mOrange and label separate populations of neurons with a vector expressing GFP alone or GFP plus Fer shRNA, and we cultured mixtures of these neurons to examine the consequences of Fer knockdown in presynaptic neurons on the spine density in postsynaptic WT neurons (Fig. S4, available at http://www.jcb.org/cgi/content/full/jcb.200807188/DC1). The density of contacts/crossings between GFP-labeled axons and mOrange-labeled dendrites was not significantly reduced by presynaptic knockdown of Fer (Fig. 3 E). In contrast, the density of dendritic spines in the WT neurons was reduced by 40% upon knockdown of presynaptic Fer (Fig. 3 D). Thus, the data suggest that depletion of presynaptic Fer inhibits postsynaptic dendritic spine morphogenesis.

Fer deficiency results in decreased synaptic vesicle cycling

To determine whether the structural defects caused by Fer deficiency impair presynaptic function, we examined potential effects of Fer knockdown on synaptic vesicle cycling. First we used FM4-64, which is accumulated in internalized recycling membrane compartments (Cochilla et al., 1999). The percentage of the synaptophysin-GFP domain that was associated with FM4-64 was reduced by ~30% in the axons of Fer shRNA–treated neurons, indicating that Fer depletion reduces the efficiency of synaptic vesicle recycling (Fig. 3, F and G). To examine whether synaptic vesicle exocytosis was inhibited, we used the pH-sensitive GFP (pHluorin) fused to the extracellular domain of the synaptic vesicle protein vGlut1 (Voglmaier et al., 2006). We coexpressed vGlut1-pHluorin with synaptophysin-mOrange to compare the distributions of total synaptic vesicles with surface synaptic vesicle proteins. To quantify the intensity and pattern of vGlut1-pHluorin and synaptophysin-mOrange puncta, we averaged the intensity every 0.01 µm along the major axis of each puncta. In control neurons, puncta of vGlut1-pHluorin–dependent fluorescence colocalized with synaptophysin-mOrange puncta. (Fig. 3, I and J). In Fer-deficient neurons, synaptic vesicles are less tightly clustered, so synaptophysin-mOrange puncta are broader with lower peak intensities (Fig. 3 J). However, the surface fluorescence of the vGlut1-pHluorin was greatly reduced in these axons (Fig. 3, H and I; Mitchell and Ryan, 2004). Thus, depletion of Fer appears to impair severely spontaneous synaptic vesicle exocytosis.

Depletion of presynaptic Fer inhibits evoked excitatory synaptic transmission

To further characterize the role of Fer in synaptic function, we performed dual-cell patch clamp recordings. We transiently depolarized a transfected neuron (vector or Fer shRNA transfected) and measured evoked excitatory postsynaptic currents (EPSCs [eEPSCs]) in an adjacent untransfected neuron (WT). In contrast to the robust eEPSCs triggered by control presynaptic neurons (Fig. 4 A), the eEPSCs were significantly reduced or not detectable after stimulation of Fer-deficient presynaptic neurons (Fig. 4 B). The percentage of successful synaptic responses between nearby pairs of neurons was reduced from ~90% in control→WT pairs to <40% in Fer shRNA→WT pairs (Fig. 4 E). The mean amplitude of eEPSCs from detectable responses was also reduced ~10-fold in shRNA→WT pairs compared with Vec→WT pairs (Fig. 4 C), and the variability of responses was increased dramatically (Fig. 4 D). Postsynaptic expression of Fer shRNA alone had no significant effect on the percentage of synaptically connected pairs of neurons (Fig. 4 E), on the mean amplitude of eEPSC (Fig. 4 C), or on the variability of synaptic responses (Fig. 4 D). For the paired neurons with detectable synaptic transmission, we also observed a slight but significant increase in the delay of synaptic transmission in shRNA→WT pairs (5.64 ± 2.47 ms for Vec→WT [n = 15] and 8.05 ± 2.47 ms for shRNA→WT [n = 7]; P = 0.041). These results show that presynaptic depletion of Fer results in a significant reduction in synaptic transmission. We have observed similar alterations of synaptic transmission when neurons are transfected at 17 d in vitro (DIV) and recorded at 21 DIV (unpublished data).

Fer regulates β-catenin phosphorylation during presynaptic development

The impaired localization of synaptic vesicle clusters in Fer-deficient neurons is similar to the phenotype observed in neurons lacking β-catenin (Bamji et al., 2003). Fer has been shown to either increase or decrease the phosphorylation of β-catenin depending on cell type (Piedra et al., 2003; Xu et al., 2004). To determine whether Fer regulates β-catenin phosphorylation in hippocampal neurons, we used lentiviruses to overexpress WT or kinase-dead Fer and examined tyrosine phosphorylation of β-catenin. Overexpression of kinase-dead Fer resulted in

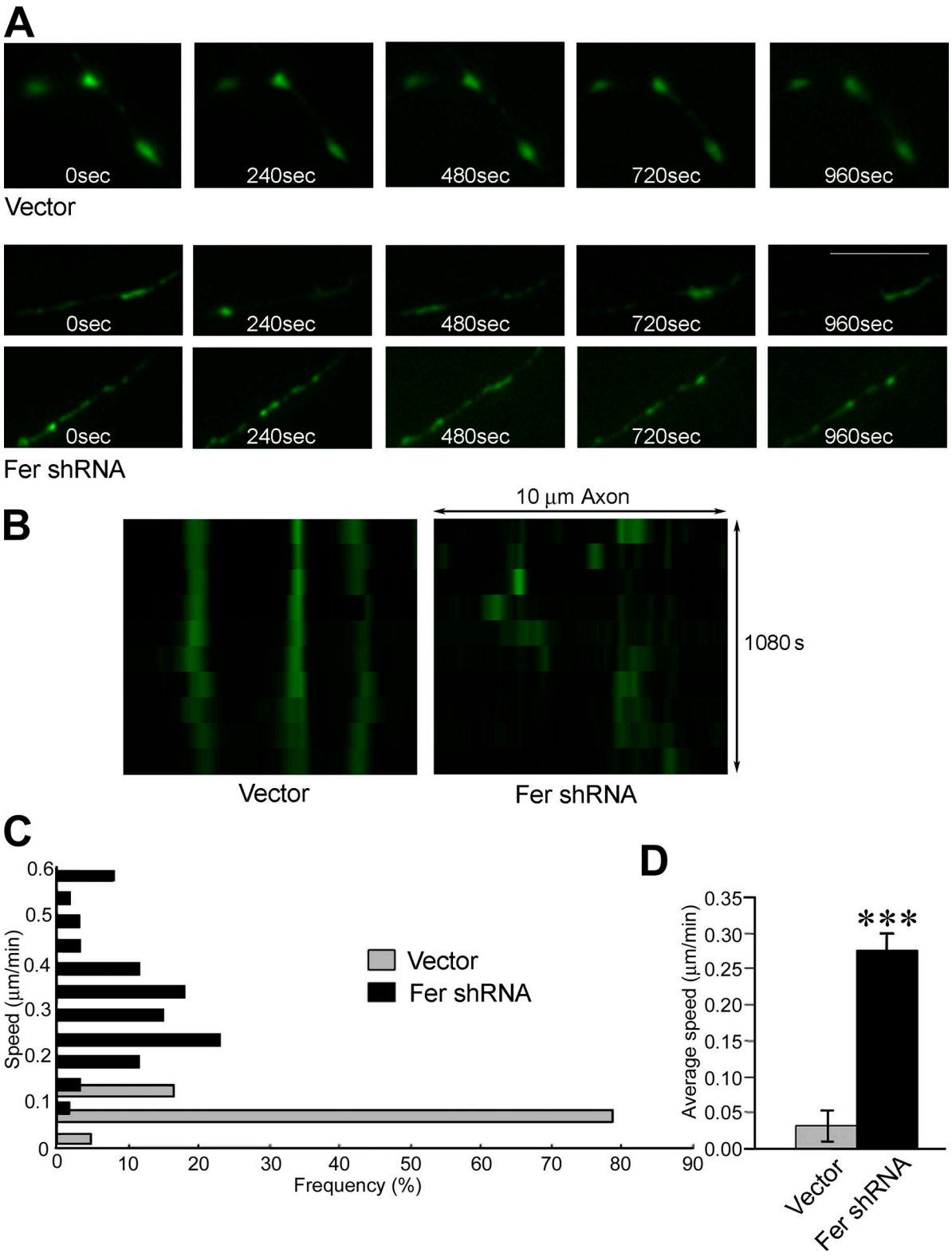

Figure 2. **Depletion of Fer increased the dynamics of synaptic vesicle puncta movement.** (A) Live cell imaging of 14 DIV cultured hippocampal neurons that were transfected at 10 DIV with synaptophysin-GFP together with control or Fer shRNA vector. Images were captured every 60 s, and frames at 240-s intervals from one representative control and two Fer shRNA–transfected neurons are presented. (B) Kymographs represent the movement of synaptophysin-GFP along the axons. (C) A histogram represents the distribution of the speed of individual synaptophysin-GFP puncta. (D) Mean speeds of synaptophysin-GFP puncta in axons of control and shRNA-transfected neurons. $n = 61$ for each condition. ***, $P < 0.0001$. Error bars represent SEM. Bar, 5 μm.

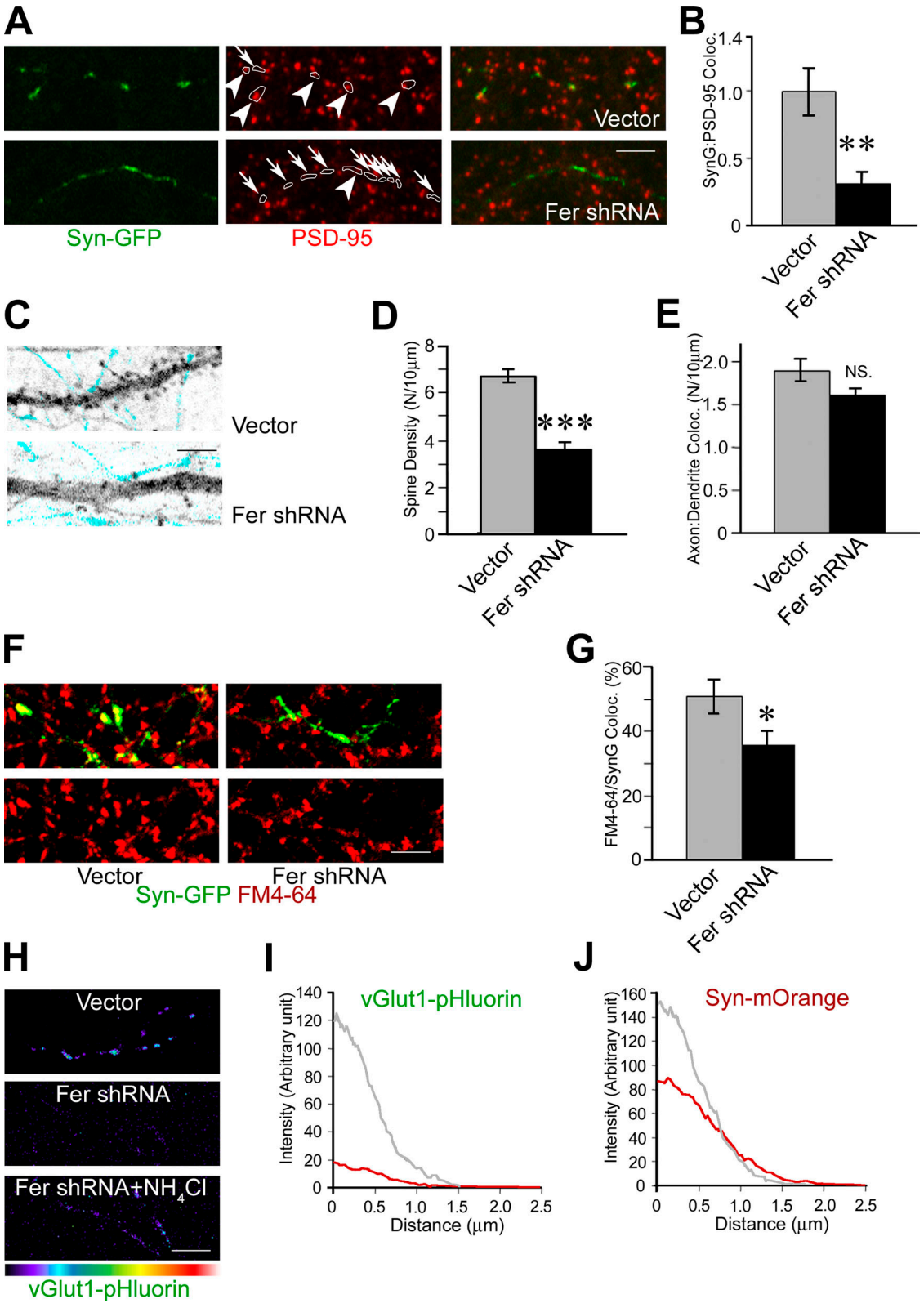

Figure 3. **Excitatory synapse formation and dendritic spine morphogenesis were reduced after presynaptic Fer deficiency.** (A) Localization of synaptophysin-GFP (Syn-GFP) and PSD-95 in hippocampal neurons transfected at 10 DIV with synaptophysin-GFP together with control or Fer shRNA. White outlines indicate the localization of synaptophysin-GFP clusters. Arrowheads indicate PSD-95 puncta colocalizing with synaptophysin-GFP puncta. Note the reduced colocalization of PSD-95 immunoreactive puncta at synaptophysin puncta in Fer shRNA–transfected neurons (arrows). (B) The fractional coverage by PSD-95 of synaptophysin-GFP puncta. The proportion of the coverage of major axis was normalized to that of the control vector–transfected neurons. n = 9 (vector) and 10 (Fer shRNA). (C) Representative images of presynaptic control or Fer shRNA vector–transfected neurons visualized with GFP (blue) and postsynaptic mOrange-transfected neurons (black). (D) Spine density of mOrange-positive neurons. Spine numbers along 10-μm dendrites of mOrange-positive dendrites. n = 18 (vector) and 19 (Fer shRNA). (E) The number of GFP-positive axons overlapping mOrange-positive dendrites per

elevated tyrosine phosphorylation of β-catenin (Fig. 5 A). In addition, overexpression of WT β-catenin or β-catenin Y654F, a mutant that prevents phosphorylation at a site known to regulate the interaction of cadherins with β-catenin, prevented the dispersion of synaptic vesicle clusters caused by overexpression of kinase-dead Fer (Fig. 5, B and D). Similarly, the impaired localization of synaptic vesicles observed in Fer shRNA–transfected neurons was suppressed by overexpression of β-catenin or β-catenin Y654F (Fig. 5, C and E). Quantification indicated that the intensity of synaptophysin-GFP puncta was not increased relative to controls after overexpression of WT or Y654F β-catenin in Fer knockdown cells (unpublished data).

To determine whether Fer-mediated regulation of synaptic vesicle cluster localization requires β-catenin, a β-catenin–specific shRNA was used to reduce β-catenin levels. As expected (Bamji et al., 2003), this resulted in dispersion of synaptic vesicle clusters, and overexpression of Fer did not prevent the dispersion of synaptic vesicles observed in β-catenin–deficient neurons (Fig. 5, F and G). Together, the results define an intracellular signaling pathway in which Fer-mediated regulation of β-catenin phosphorylation controls localization of synaptic vesicles.

Deletion of p120ctn prevents normal synaptic vesicle localization

Prior work has shown that Fer must bind p120ctn to promote β-catenin binding to N-cadherin in neuroepithelial cells of the chick retina (Xu et al., 2004). To determine whether Fer-mediated promotion of synaptic vesicle cluster formation requires p120ctn, we grew hippocampal neurons from a *p120ctn*$^{fl/fl}$ mouse described previously (Elia et al., 2006) and deleted *p120ctn* in cultured *p120ctn*$^{fl/fl}$ neurons by transfection with a Cre recombinase. In these neurons, synaptophysin-GFP puncta were diffuse and poorly localized, which is similar to observations in Fer-deficient neurons (Fig. 6, A and B).

Inhibition of Fer binding to p120ctn prevents normal synaptic vesicle localization

To determine more directly whether association with p120ctn is important for Fer-mediated promotion of synaptic vesicle localization, we exposed neurons to a cell-permeable peptide previously shown to inhibit p120ctn–Fer association (FerP), corresponding to aa 331–360 of Fer (Xu et al., 2004). Application of FerP prevented the normal localization of both synaptic vesicles and Bassoon-containing clusters (Fig. 6, C–F). Synaptic vesicle clusters in FerP-treated neurons were highly unstable with random and undirected movements (Fig. 6, G and H; and Videos 4 and 5, available at http://www.jcb.org/cgi/content/full/jcb.200807188/DC1). FerP treatment dramatically increased tyrosine phosphorylation of β-catenin, suggesting that the association of Fer with p120ctn reduces β-catenin phosphorylation during presynaptic development (Fig. 6 I). We overexpressed a mutant of p120ctn lacking a sequence for Fer binding (p120Δ131–156) and also observed impaired synaptic vesicle localization in transfected axons (Fig. 7 C), suggesting that the Fer interaction site in p120ctn is required for presynaptic development.

The Fer interaction site in p120ctn also mediates binding to RhoA, but RhoA does not mediate the misregulation of synaptic vesicle cluster localization

In prior work, it has been shown that the N-terminal domain of p120ctn interacts with RhoA and is one of two sites in p120ctn required for p120ctn to function as a Rho–GDP dissociation inhibitor (Anastasiadis, 2007; Castano et al., 2007; Yanagisawa et al., 2008). A RhoA-binding domain has been mapped to the N-terminal region (aa 102–234) of p120ctn (Castano et al., 2007), raising the possibility that the phenotypes observed after FerP application and p120Δ131–156 overexpression may reflect perturbations of Rho, not Fer, activity. We examined whether the Fer-binding sequence in p120ctn also mediates binding to RhoA. In an in vitro binding assay, this sequence alone was able to pull down RhoA (Fig. 7, A and B). To determine whether failure of p120Δ131–156 to function as a Rho–GDP dissociation inhibitor could explain the impaired localization of synaptic vesicles after overexpression of this mutant, we coexpressed with p120Δ131–156, a dominant-negative RhoA mutant (T19N). Suppression of RhoA activity by dominant-negative RhoA did not suppress the reduced synaptic vesicle clustering observed as a result of overexpression of p120Δ131–156. Overexpression of a constitutively active RhoA mutant (G14V) also failed to inhibit synaptic vesicle localization (Fig. 7, C and D). Both experiments argue that the diffusion of presynaptic clusters caused by inhibition of the Fer–p120ctn interaction did not result from deregulated presynaptic Rho activity even though Fer and RhoA share a binding site in p120ctn.

SHP-2 is regulated by Fer and dephosphorylates β-catenin in presynaptic development: differential roles of tyrosine phosphatases

The paradoxical observation that inhibition of a tyrosine kinase, Fer, results in elevated tyrosine phosphorylation of β-catenin implies that Fer is acting indirectly through inactivation of a tyrosine kinase or activation of a protein tyrosine phosphatase. In prior work, it has been shown in chick retinal neuroepithelial cells that

mOrange-positive dendrite length. *n* = 11 (vector) and 12 (Fer shRNA). NS, P = 0.058. (F) Imaging at 14 DIV of hippocampal neurons transfected at 10 DIV with synaptophysin-GFP together with control or Fer shRNA vector. Cells were loaded with FM4-64 (red) at 14 DIV. (G) The percent coverage by FM4-64 of synaptophysin-GFP puncta length. *n* = 9 (vector) and 8 (Fer shRNA). (H) Imaging of vGlut1-pHluorin in 14 DIV hippocampal neurons transfected at 10 DIV with vGlut1-pHluorin, synaptophysin-mOrange (not depicted), and control or Fer shRNA. The vGlut1-pHluorin signal has been processed to indicate signal intensity. After initial imaging, cells were treated with NH_4Cl to elevate the pH of internal vesicles to pH 7.4 using NH_4Cl, which revealed the presence of vGlut1-pHluorin puncta in Fer-deficient synaptophysin-mOrange–positive neurons, confirming that the low intensity was not caused by a failure in transfection or protein expression. (I and J) Graph lines indicating mean fluorescence intensities at denoted distances from the centers of the vGlut1-pHluorin puncta (I) and synaptophysin-mOrange (Syn-mOrange) puncta (J). Gray lines indicate control vector–transfected conditions, whereas red lines indicate Fer shRNA–transfected conditions. *n* = 30 (vector) and 57 (Fer shRNA). *, P < 0.05; **, P < 0.01; ***, P < 0.0001. Error bars represent SEM. Bars, 5 µm.

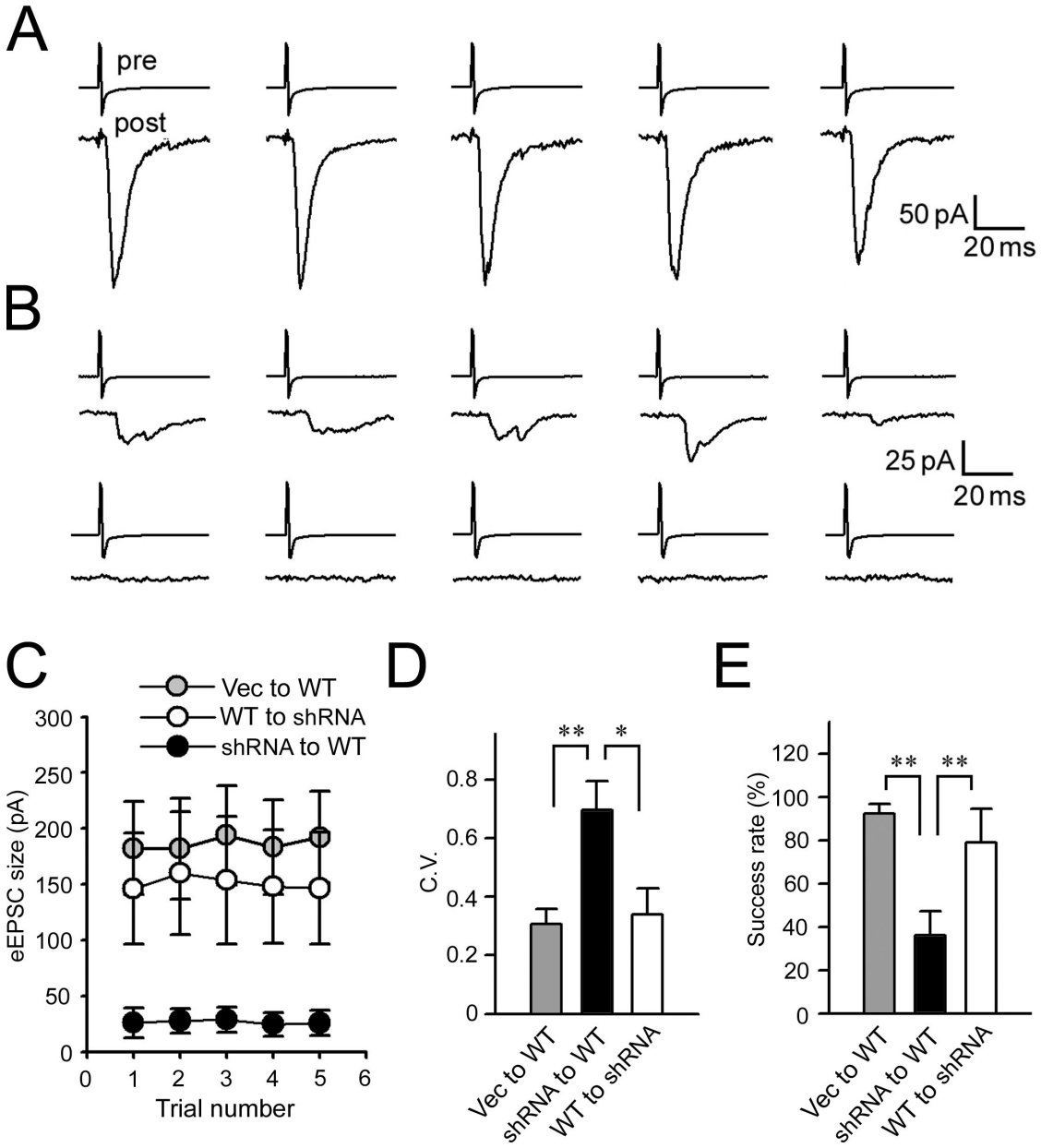

Figure 4. **Presynaptic Fer-mediated eEPSCs.** Paired neurons with soma–soma distance around 100 µm were selected for dual recording. Neurons expressing control (Vec) or Fer shRNA (shRNA) were identified by the expression of GFP, which is contained in the same constructs. Non-GFP–expressing neurons were considered as WT. Recordings were performed at 14–17 DIV. (A) Persistent eEPSCs at vector to WT synapses. Five constant stimuli (200 mV for 1 ms) delivered into the presynaptic cell (pre) reliably evoke robust EPSCs at the postsynaptic cell (post). The time interval between stimuli is 10 s. (B) Examples of eEPSCs at Fer shRNA to WT synapse. Unlike the control, stimuli with the same strength delivered at Fer shRNA neurons initiate only weak or no eEPSCs by neighboring WT neurons. (C) Substantial reduction of EPSC size by presynaptic Fer shRNA. Lines and circles indicate the average values from five stimulation trials. It is worth noting that postsynaptic knockdown of Fer (i.e., WT to Fer synapses) does not have a statistically significant effect on the eEPSC amplitude. (D) Increased variation on the EPSC amplitude at Fer shRNA to WT synapses. C.V., coefficient of variation. (E) Low success rate of the synaptic transmission rate at Fer shRNA to WT synapses. Synaptic transmission is defined as successful when an evoked response is five times larger than the root mean square of the noise (~10–13 pA). n = 20 (vector→WT), 15 (shRNA→WT), and 8 (WT→shRNA). *, $P < 0.025$; **, $P < 0.01$; one-way analysis of variance. Error bars indicate SEM.

Fer phosphorylates PTP1B, which increases the association of this protein phosphatase with the cadherin complex, thereby reducing the phosphorylation of β-catenin (Xu et al., 2004). Motivated by these observations, we first determined whether PTP1B regulates synaptic vesicle cluster localization. Contrary to expectation, shRNA-mediated depletion of PTP1B did not inhibit synaptic vesicle clustering (Fig. 8, A and D; and Fig. S5, available at http://www.jcb.org/cgi/content/full/jcb.200807188/DC1).

SHP-2 is another protein tyrosine phosphatase expressed in hippocampal neurons that has been shown in some cell types to regulate phosphorylation of β-catenin and other constituents of the cadherin complex (Ukropec et al., 2000; Sallee et al., 2006; Kim et al., 2007). We observed that SHP-2 shRNA–mediated knockdown severely impaired synaptic vesicle localization, which is similar to observations in Fer-deficient neurons (Fig. 8, B and E; and Fig. S5). Overexpression in SHP-2–deficient

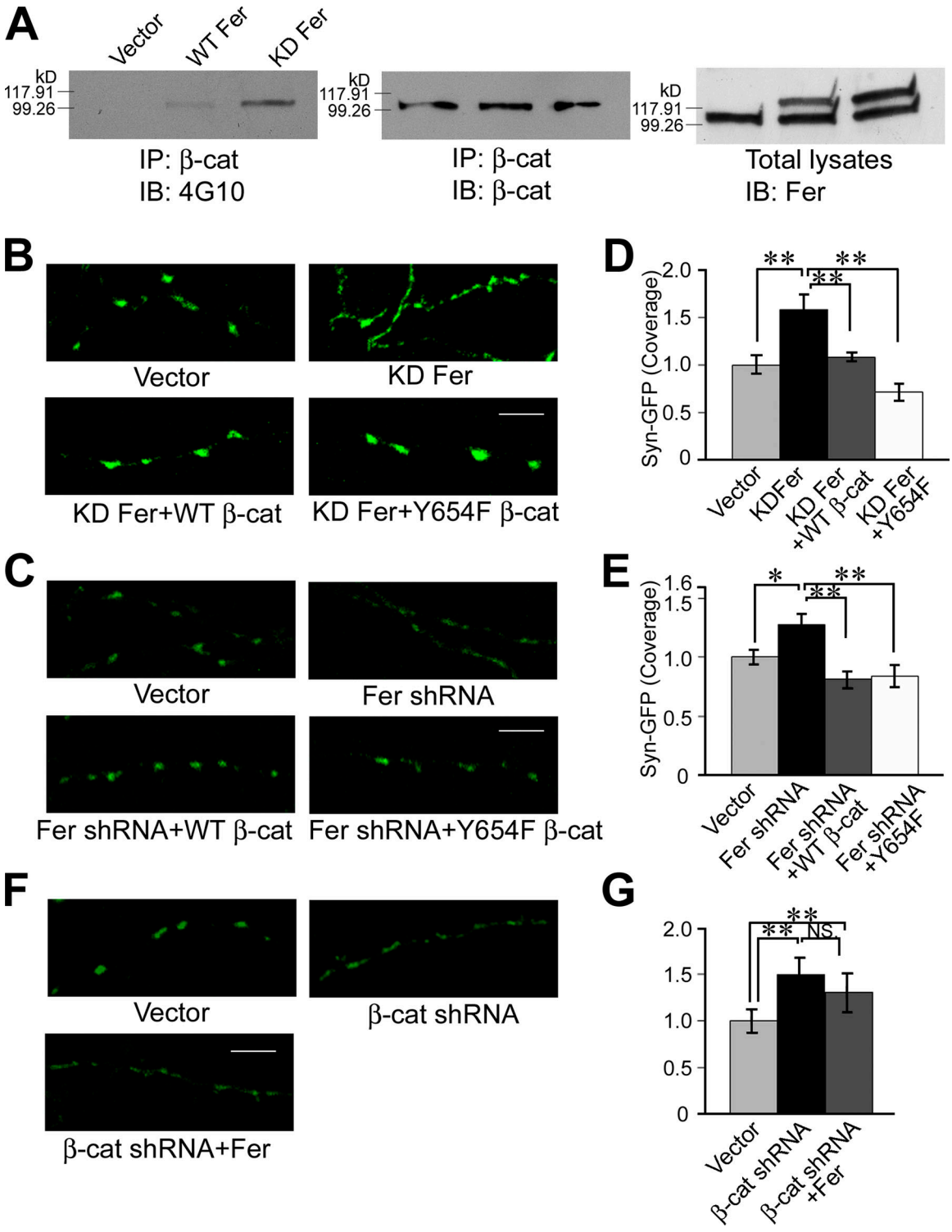

Figure 5. **β-Catenin overexpression suppresses Fer-mediated synaptic vesicle delocalization.** (A) Phosphorylation of β-catenin (β-cat) is increased after inhibition of Fer function. 7 DIV rat cortical neurons were infected with lentiviruses expressing WT Fer or KDFer. At 14 DIV, extracts were prepared and used for IP with anti–β-catenin followed by immunoblotting (IB) with antiphosphotyrosine antibody 4G10 (left), and the blots were reprobed with anti–β-catenin (middle). Total lysates were immunoblotted with anti-Fer to examine the expression of exogenous Fer (right). (B–E) Expression of WT or Y654F β-catenin prevents synaptic puncta dispersion caused by inhibition of Fer. Hippocampal neurons were transfected with synaptophysin-GFP (Syn-GFP) together with the indicated DNAs at 10 DIV and were fixed at 14 DIV for imaging. Representative images are shown in B and C. Normalized coverage of synaptophysin-GFP per 10 μm of axon in each condition is quantified in D and E. In D, $n = 8$ (vector), 9 (KDFer), 8 (KDFer + WTβ-cat), and 7 (KDFer + Y654Fβ-cat). In E, $n = 15$ (vector), 21 (Fer shRNA), 11 (Fer shRNA + WTβ-cat), and 14 (Fer shRNA + Y654Fβ-cat). (F and G) Delocalization of presynaptic puncta by β-catenin knockdown was not rescued by overexpression of Fer. Hippocampal neurons were transfected with the indicated DNAs at 10 DIV and fixed at 14 DIV for imaging. Representative images of synaptophysin-GFP clusters in each condition are shown in F, and normalized coverage of synaptophysin-GFP per 10-μm axon in condition is presented in G. $n = 13$ (vector), 16 (β-cat shRNA), and 10 (β-cat shRNA + Fer). KDFer, kinase-dead mutant (K591R) of Fer. *, $P < 0.05$; **, $P < 0.01$. Error bars represent SEM. Bars, 5 μm.

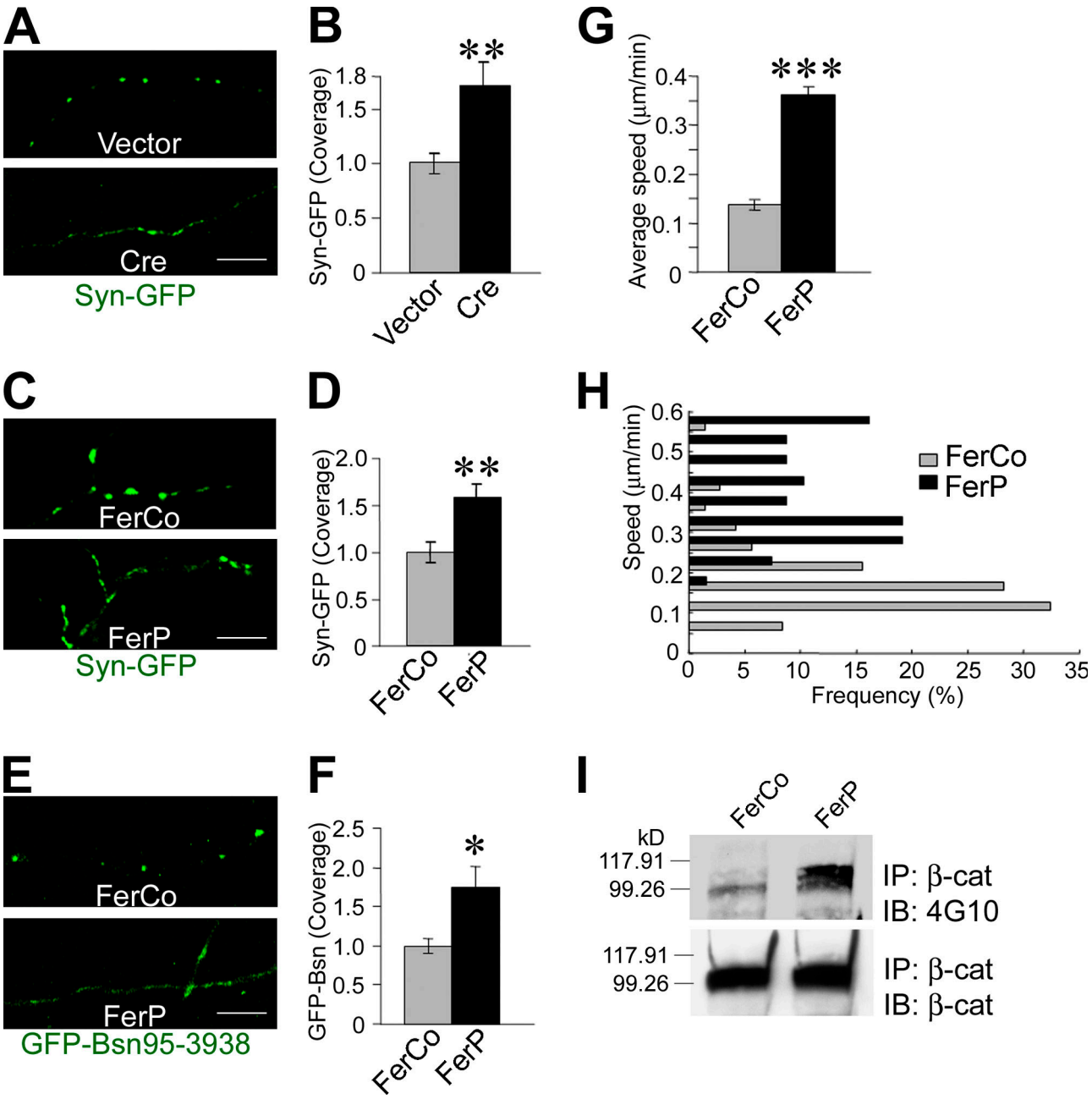

Figure 6. **Requirement for interaction between Fer and p120ctn to regulate β-catenin phosphorylation and synaptic vesicle localization.** (A and B) Hippocampal neurons from postnatal day 0 *p120ctn*$^{fl/fl}$ mice were transfected with vector or Cre recombinase together with synaptophysin-GFP (Syn-GFP) at 10 DIV and were fixed at 14 DIV for imaging. Representative synaptophysin-GFP patterns are shown in A, and normalized coverage of synaptophysin-GFP in each condition is shown in B. $n = 9$ (vector) and 11 (Cre). (C–F) Imaging at 13 DIV of rat hippocampal neurons that were transfected at 10 DIV with synaptophysin-GFP (C and D) or GFP–Bsn95-3938 (E and F). Cultures were incubated with 5 µg/ml FerCo or FerP from 11 to 13 DIV. The coverage (micrometers of GFP per 10 µm of axon) of synaptophysin-GFP ($n = 10$ [FerCo] and 12 [FerP]) or GFP–Bsn-95-3938 ($n = 8$ [FerCo] and 9 [FerP]) is quantified in D and F. (G and H) Time-lapse analysis at 13 DIV of synaptophysin-GFP–expressing organelles in hippocampal neurons transfected at 10 DIV. Cultures were treated with FerCo or FerP for 2 h before time-lapse imaging. Pictures were taken every 1 min. Increased movements of puncta are observed in FerP-treated neurons compared with FerCo-treated control neurons. The average speeds of individual synaptophysin-GFP puncta in each condition are shown in G, and a histogram representing the distribution of the speeds of each puncta is shown in H. $n = 71$ (FerCo) and 68 (FerP). (I) 12 DIV hippocampal neurons were treated with FerCo or FerP for 4 h followed by IP with anti–β-catenin (β-cat) and immunoblotting (IB) with antiphosphotyrosine mAb 4G10 (top). The blot was reprobed with anti–β-catenin (bottom). FerCo, control peptide; FerP, Fer peptide. *, $P < 0.05$; **, $P < 0.01$; ***, $P < 0.0001$. Error bars represent SEM. Bars, 5 µm.

neurons of WT β-catenin or β-catenin Y654F restored normal synaptic vesicle localization. In addition, the tyrosine phosphorylation of β-catenin was significantly increased after knockdown of SHP-2, confirming a role for this phosphatase in control of β-catenin tyrosine phosphorylation (Fig. 8 G). Next, we examined whether Fer is functionally linked to SHP-2 by expressing a constitutively active mutant (E76K) of SHP-2. Overexpression of constitutively active SHP-2 restored synaptic vesicle localization

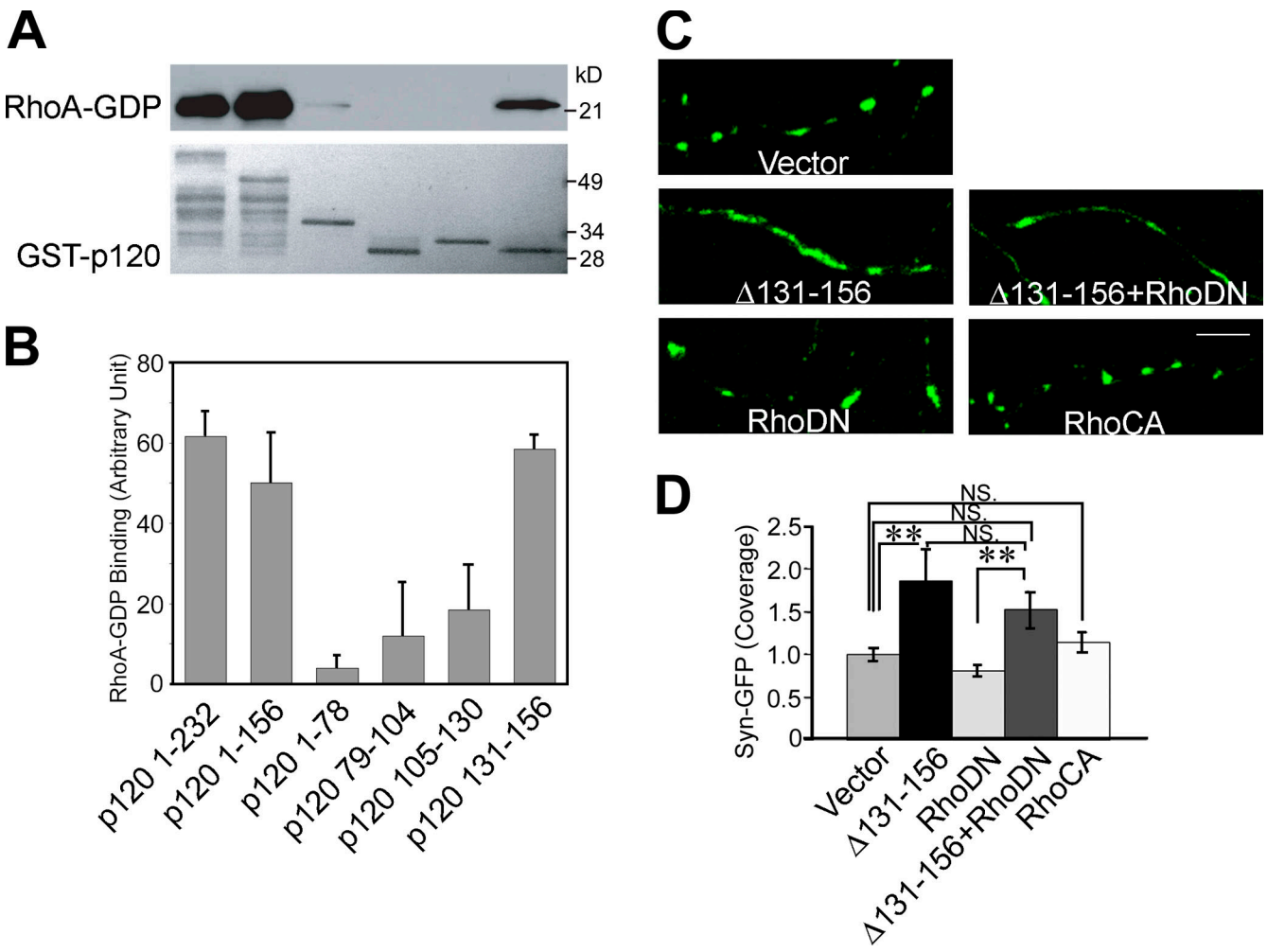

Figure 7. **The Fer-binding region in p120ctn overlaps with a RhoA-binding site, but the synaptic diffusion phenotype is independent of Rho regulation.** (A and B) In vitro binding assay to map RhoA and p120ctn interaction sites. Recombinant GST-p120ctn peptides corresponding to the indicated aa were incubated with GDP-bound recombinant RhoA. (A) Representative images of RhoA-GDP bound to GST-p120ctn. The amounts of RhoA-GDP bound to GST-p120ctn were quantified in B. (C and D) Visualization of synaptophysin-GFP (Syn-GFP) at 14 DIV in neurons transfected at 10 DIV with synaptophysin-GFP together with the indicated constructs. Neurons were analyzed for the synaptophysin-GFP coverage (micrometers of GFP per 10 µm of axon length normalized to control). *n* = 16 (vector), 16 (Δ131–156), 18 (RhoDN), 17 (Δ131–156 + RhoDN), and 9 (RhoCA). Δ131–156, 131–156 aa-deleted p120ctn. RhoDN, dominant-negative mutant (T19N) RhoA; RhoCA, constitutively active mutant (G14V) RhoA. **, $P < 0.01$. Error bars represent SEM. Bar, 5 µm.

in Fer-deficient neurons (Fig. 8, C and F). Collectively, the data suggest that Fer may control synaptic vesicle localization through regulation of SHP-2 and suggest further that it may act through inhibition of β-catenin tyrosine phosphorylation.

Discussion

Current results indicate that the cytoplasmic tyrosine kinase Fer promotes differentiation of the presynaptic compartment in hippocampal neurons. In addition to cell-autonomous regulation of presynaptic differentiation, presynaptic Fer is required for postsynaptic spine differentiation and normal excitatory transmission. Genetic deletion of p120ctn, inhibition of p120ctn–Fer association, and shRNA-mediated depletion of Fer or SHP-2 each prevented normal synaptic vesicle localization at synapses. These perturbations resulted in elevated tyrosine phosphorylation of β-catenin. Overexpression of β-catenin or β-catenin Y654F prevented the mislocalization of synaptic vesicles. A model of the presynaptic Fer–p120ctn–SHP-2–β-catenin mediated signaling pathway leading to synaptic development is presented in Fig. 9.

Presynaptic Fer is required for presynaptic assembly, excitatory synapse formation, postsynaptic spine morphogenesis, and synaptic function

Results from fixed cell imaging and time-lapse imaging of live cells demonstrate that Fer kinase is needed for proper localization and stabilization of synaptic vesicle clusters. In central nervous system synaptogenesis, it is now believed that presynaptic components are transported in multimolecular complexes. A key feature of presynaptic development is the proper localization of these complexes to synaptic sites. Components of the CAZ are transported as constituents of Piccolo–Bassoon transport vesicles, which are inserted into the plasmalemma to form presynaptic active zones, after which additional scaffold proteins and synaptic vesicles are recruited to these sites through poorly

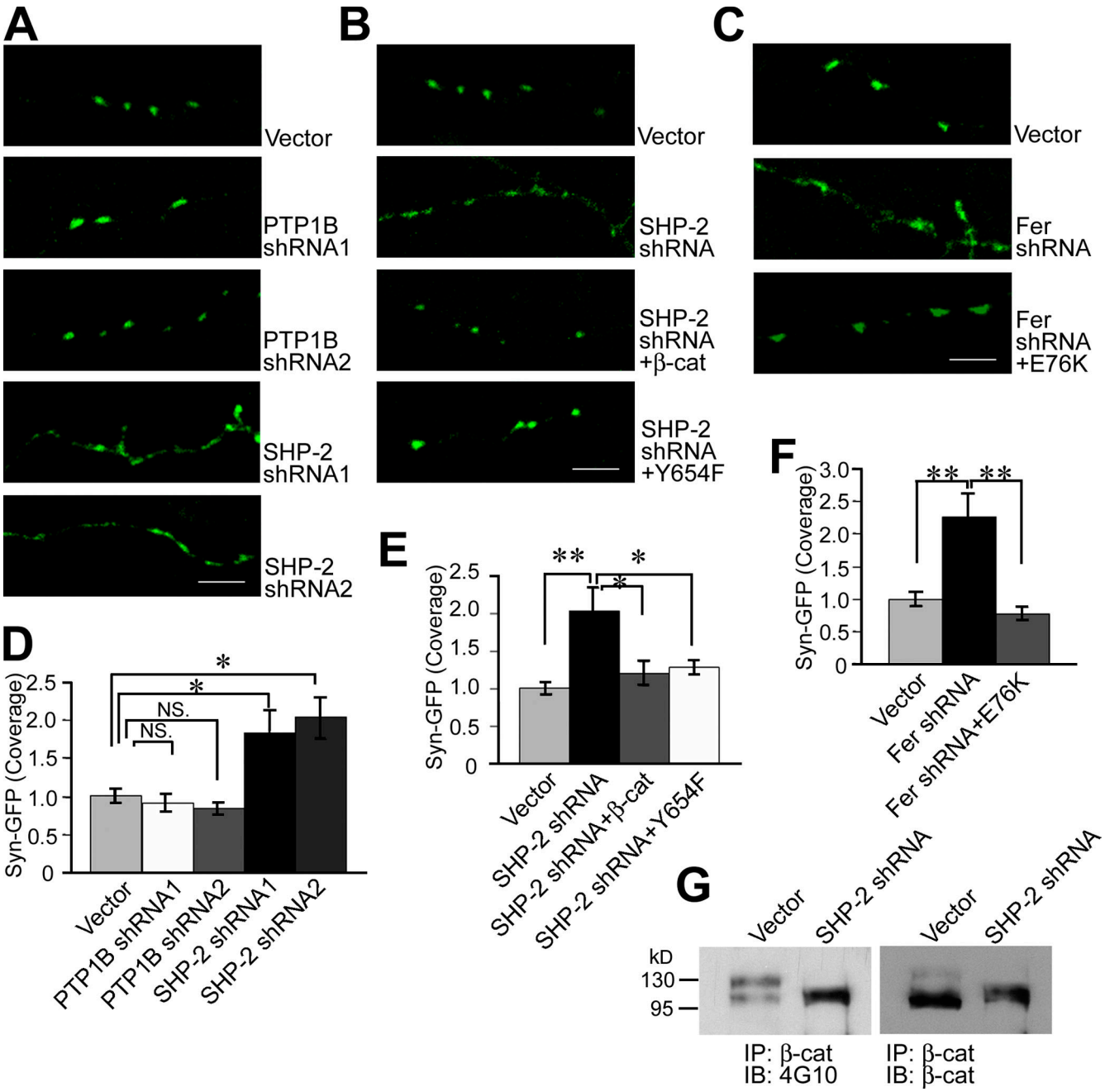

Figure 8. **SHP-2 is downstream of Fer in mediating β-catenin regulation during presynaptic development.** (A–F) Effects of PTP1B and SHP-2 depletion on synaptic vesicle localization and suppression of SHP-2 phenotype by overexpression of β-catenin (β-cat) and β-catenin Y654F. 14 DIV hippocampal neurons were imaged at 14 DIV after transfection at 10 DIV with synaptophysin-GFP (Syn-GFP) together with the indicated constructs. Quantification of the synaptophysin-GFP coverage (normalized micrometers of GFP per 10 µm of axon length) is presented in D–F. SHP-2 shRNA1 was used for all experiments in B, E, and G. In D, n = 22 (vector), 26 (PTP1B shRNA1), 6 (PTP1B shRNA2), 10 (SHP-2 shRNA1), and 6 (SHP-2 shRNA2). In E, n = 12 (vector), 13 (SHP-2 shRNA), 11 (SHP-2 shRNA + β-catenin), and 13 (SHP-2 shRNA + Y654F). In F, n = 11 (vector), 11 (Fer shRNA), and 10 (Fer shRNA + E76K). (G) Increased phosphorylation of β-catenin in SHP-2–depleted neurons. Rat hippocampal neurons were transfected by electroporation before plating and at 14 DIV were lysed and immunoprecipitated with anti–β-catenin. Blots were probed with antiphosphotyrosine mAb 4G10 (left) followed by reprobing with anti–β-catenin. IB, immunoblotting. *, $P < 0.05$; **, $P < 0.01$. Error bars represent SEM. Bars, 10 µm.

understood mechanisms (Bresler et al., 2004; McAllister, 2007). Localization of components of the active zone cytoplasmic matrix as well as synaptic vesicles requires normal Fer function.

The impairments in synaptic vesicle and active zone localization after presynaptic depletion of Fer resulted in a striking reduction in spine morphogenesis within juxtaposed dendrites. Reciprocal signaling interactions between pre- and postsynaptic compartments are clearly required for normal synapse formation (Okabe et al., 2001; Tada and Sheng, 2006; Lardi-Studler and Fritschy, 2007). Numerous observations implicate cell adhesion–mediated interactions in synapse localization and differentiation (Yamada and Nelson, 2007). For example, N-cadherin promotes spine morphogenesis and stability in cooperation with p120ctn, αN-catenin, leukocyte common antigen–related protein,

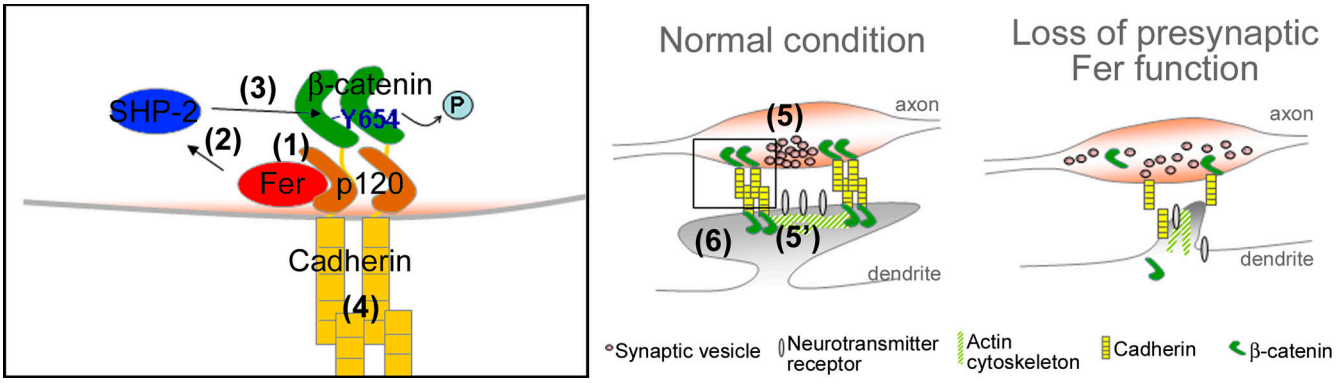

Figure 9. **Proposed intracellular signaling involving Fer, p120ctn, SHP-2, β-catenin, and cadherin during synaptic development.** Based on the results and current knowledge, we propose a signaling cascade (1–4) leading to synaptic formation (5 and 6). The model focuses on the role of Fer and cadherin components at the presynaptic compartment (left). (1) Fer is recruited by p120ctn to the cadherin complex. (2) Fer acts on SHP-2 tyrosine phosphatase to increase the phosphatase activity at the cadherin complex. This may be done in two ways that need to be characterized further: Fer may increase phosphorylation or modify the protein interaction of SHP-2, thereby increasing the phosphatase activity of SHP-2, or Fer enhances the recruitment of SHP-2 to the cadherin complex. (3) SHP-2 dephosphorylates β-catenin to strengthen the interaction between cadherin and β-catenin. (4) Cadherin adhesion and possibly other cell adhesion regulated by cadherin (e.g., nectin-mediated adhesion) are stabilized. Through this cadherin–catenin adhesion complex (5) in the presynaptic compartment, β-catenin acts as a scaffold using its PSD-95/disc large/ZO-1–binding domain to trap and stabilize the synaptic vesicles at the synaptic site. (5′) In the postsynaptic compartment, dendritic spine morphogenesis and recruitment of postsynaptic components are proceeded to form a mature and functional synapse (6). If this sequence is perturbed by deficiency of presynaptic Fer, we imagine the presynaptic vesicles will be scattered, and the disrupted integrity of cadherin–catenin will result in a failure in synapse formation and function (right).

and GluR2 (Togashi et al., 2002; Dunah et al., 2005; Elia et al., 2006; Saglietti et al., 2007). It is possible that this trans-synaptic effect of Fer deficiency is at least in part mediated through reduced postsynaptic N-cadherin function.

As assessed by imaging of FM4-64 uptake, pH-sensitive GFP monitoring of exocytosis, and electrophysiological recordings, synaptic function is severely perturbed by Fer deficiency. This may be caused by (a) deficits in excitatory synapse formation, (b) reduced size of synaptic vesicle pools, and/or (c) changes in the structure and function of the presynaptic active zone. Consistent with the first possibility are our results showing reduction in PSD-95 immunoreactivity and dendritic spine density. The observed reduction in EPSC amplitude may also reflect these postsynaptic abnormalities. Reduced numbers of synaptic vesicles are also likely to contribute to the reduced size of evoked responses observed after Fer depletion from presynaptic terminals. Interestingly, in our prior study, depletion of β-catenin resulted in a reduced reserve vesicle pool size without reducing the size of the readily releasable vesicle pool (Bamji et al., 2003). In future studies, it will be interesting to examine the role of the p120ctn–Fer–SHP-2 pathway in controlling calcium influx and clearance, paired-pulse facilitation and depression, and other aspects of synaptic function and plasticity.

Signaling pathways mediating Fer function in synaptic development

Regulation of phosphorylation of β-catenin appears to be a significant downstream target of Fer. X-ray structural analysis, in vitro binding assays, and analyses of cellular immunoprecipitates have shown that type I cadherin-promoted stable cell–cell junction formation requires β-catenin. Phosphorylation of β-catenin controls its interactions with cadherins and other binding partners (Huber and Weis, 2001; Lilien and Balsamo, 2005; Xu and Kimelman, 2007). Studies have revealed that phosphorylation of either Y489 or Y654 reduces the interactions between cadherins and β-catenin, whereas phosphorylation of Y142 reduces interactions between α- and β-catenin (Roura et al., 1999; Huber and Weis, 2001; Piedra et al., 2003; Rhee et al., 2007).

Interestingly, prior observations indicate that Y654 phosphorylation controls synaptic vesicle localization, spine morphogenesis, AMPA (α-amino-3-hydroxy-5-methyl-4-isoxazolepropionic acid) receptor turnover, and synaptic function. Brain-derived neurotrophic factor–stimulated phosphorylation of Y654 reduces cadherin–β-catenin association and synaptic vesicle cluster stability and promotes new synapse formation (Bamji et al., 2006). Synaptic activity acting through suppression of Cdk5 reduces phosphorylation of Y654, promotes localization of β-catenin to dendritic spines, increases spine size, and enhances synaptic strength (Murase et al., 2002). Recently, it has been shown that NMDA (*N*-methyl-D-aspartate) receptor–dependent long-term depression is mediated through phosphorylation of β-catenin Y654, which results in reduced cadherin–β-catenin association and elevated N-cadherin endocytosis (Tai et al., 2007). It will be interesting to study whether Fer regulates either AMPA receptor trafficking or NMDA receptor–dependent long-term depression.

It seems unlikely that phosphorylation of Y142, a site that regulates interactions with α-catenin, is involved causally in the regulation of synaptic vesicle localization downstream of Fer. First, we previously demonstrated that deletion of the α-catenin–binding site in β-catenin did not prevent synaptic vesicle localization (Bamji et al., 2003). Second, although Y142 may be phosphorylated by Fer (Piedra et al., 2003), we observed increased, not decreased, phosphorylation of β-catenin in Fer-depleted neurons.

Several phosphatases have been identified in the cadherin complex in various cell types, including SHP-1, SHP-2, PEZ, low molecular weight protein tyrosine phosphatase, PTP1B, leukocyte

common antigen–related protein, and RPTP-μ (Piedra et al., 2003; Lilien and Balsamo, 2005). In retina neuroepithelial cells, Fer appears to promote dephosphorylation of β-catenin and cadherin complex integrity through phosphorylation of PTP1B (Xu et al., 2004). In contrast, our results indicate that PTP1B is not a major regulator of β-catenin during initial synapse formation by hippocampal neurons. However, we have observed that the knockdown of PTP1B affects the maintenance of the normal synapse number in mature neurons (unpublished data). In developing hippocampal neurons, our data indicate that SHP-2 is an important negative regulator of β-catenin phosphorylation that promotes cadherin complex integrity and presynaptic terminal differentiation. Phosphorylation of Y542 and Y580 on SHP-2 increases the tyrosine phosphatase activity of SHP-2 (Mohi and Neel, 2007; Pao et al., 2007). SHP-2 has been shown to be phosphorylated by Fer and to be activated by both phosphorylation and binding of its SH2 domains to other proteins, such as Gab-1 (Kogata et al., 2003).

Our results indicate that both Fer and RhoA bind overlapping sites in the N-terminal domain of p120ctn. Our functional experiments of presynaptic assembly, however, indicate that down-regulation of Rho by p120ctn is not required for presynaptic development. In addition, overexpression of kinase-dead Fer severely impaired localization of synaptic vesicle clusters. Collectively, these observations indicate that the N terminus of p120ctn promotes synaptic terminal differentiation through recruitment of Fer, not Rho. In contrast, our previous experiments on postsynaptic spine morphogenesis demonstrated that p120ctn promotes spine formation and maturation through control of Rho family GTPases as well as enhancement of cadherin stability (Elia et al., 2006). Thus, p120ctn has important roles in both pre- and postsynaptic development but promotes differentiation of these two compartments through distinct signaling pathways.

Finally, although our experiments indicate that Fer acts through SHP-2 to control β-catenin phosphorylation and argue for an important regulatory role of β-catenin in presynaptic differentiation and function, Fer and SHP-2 have been shown to have a diversity of substrates in other cell types (Ha et al., 2008). The physiological consequences of presynaptic or postsynaptic β-catenin depletion differ substantially from our observations on synaptic transmission in neurons lacking Fer (Bamji et al., 2003; Okuda et al., 2007). In addition, localization of Bassoon is impaired in Fer-depleted neurons, although we did not observe an obvious perturbation of Bassoon localization in neurons lacking β-catenin (Bamji et al., 2003). It seems very likely that other downstream targets of Fer in addition to β-catenin will prove important in understanding the role of Fer in synapse differentiation and function.

Materials and methods

Reagents and constructs

Rabbit anti-Fer antiserum was provided by P. Greer (Queen's University, Kingston, Ontario, Canada), anti–N-cadherin was provided by D. Colman (McGill University, Montreal, Quebec, Canada), and anti–N-cadherin mAb (13A9) was provided by M. Wheelock (University of Nebraska, Omaha, NE).

Anti-p120ctn and antiphospho–SHP-2 were obtained from BD, anti–β-catenin was obtained from Invitrogen, anti–Tau-1 (MAB3420) and anti-vGlut1 were obtained from Millipore, anti-MAP2 and antisynaptophysin were obtained from Sigma-Aldrich, anti–PSD-95 was obtained from Thermo Fisher Scientific, anti-PTP1B was obtained from EMD, anti–SHP-2 was obtained from Santa Cruz Biotechnology, Inc., and antiphosphotyrosine 4G10 was obtained from Millipore. Complete Mini was purchased from Roche. Fluorescence-conjugated secondary antibodies, FM4-64, and antifade mounting solution were purchased from Invitrogen. FerP and FerCo peptides were described previously in Xu et al. (2004). Amaxa nucleofactor and its reaction reagents were obtained from Amaxa Biosystems.

Synaptophysin-GFP was provided by T. Nakata (University of Tokyo, Tokyo, Japan), GFP–Bsn-95-3938 was provided by C. Garner (Stanford University, Palo Alto, CA), vGlut1-pHluorin was provided by R.H. Edwards (University of California, San Francisco, San Francisco, CA), mOrange was provided by R.Y. Tsien (University of California, San Diego, La Jolla, CA), and synaptophysin-CFP was provided by S. Okabe (Tokyo Medical and Dental University, Tokyo, Japan). Synaptophysin-mOrange was made by replacing CFP with mOrange in synaptophysin-CFP. Lentiviral constructs were originally provided by C. Lois (Massachusetts Institute of Technology, Cambridge, MA) and I.M. Verma (Salk Institute, La Jolla, CA).

shRNA constructs were made by annealing of the following oligonucleotides and insertion into pSUPERRetro or pSUPERGFP; for β-catenin shRNA, the same target sequence (β-cat811) used by Zhang et al. (2007) was used: Fer shRNA, 5′-GATCCCCAAGGAGAGGCTATCCAAATTTGATTCAAGAGATCAAATTTGGATAGCCTCTCCTTTTTTTA-3′ and 5′-AGCTTAAAAAAAGGAGAGGCTATCCAAATTTGATCTCTTGAATCAAATTTGGATAGCCTCTCCTTGGG-3′; PTP1B shRNA2, 5′-GATCCCCCCAGGATATTCGACATGAATTCAAGAGATTCATGTCGAATATCCTGGTTTTTA-3′ and 5′-AGCTTAAAAACCAGGATATTCGACATGAATCTCTTGAATTCATGTCGAATATCCTGGGGG-3′; SHP-2 shRNA1, 5′-GATCCCCGAGGGAAGAGCAAGTGTGTTTCAAGAGAACACACTTGCTCTTCCCTCTTTTTA-3′ and 5′-AGCTTAAAAAGAGGGAAGAGCAAGTGTGTTCTCTTGAAACACACTTGCTCTCCCTCGGG-3′; and SHP-2 shRNA2, 5′-GATCCCCGGACATGAATATACCAATATTCAAGAGATATTGGTATATTCATGTCCTTTTTA-3′ and 5′-AGCTTAAAAAGGACATGAATATACCAATATCTCTTGAATATTGGTATATTCATGTCCGGG-3′. PTP1B shRNA1 was made by annealing the following oligonucleotides and insertion into pLentiLox3.7: 5′-TCGAGCAGATCGATAAGGCTTTCAAGAGAAGCCTTATCGATCTGCTCGTTTTTTG-3′ and 5′-TCGACAAAAAACGAGCAGATCGATAAGGCTTCTCTTGAAAGCCTTATCGATCTGCTCGA-3′.

shRNA-resistant constructs were made by site-directed mutagenesis using QuikChange Mutagenesis (Agilent Technologies) using the following primers: Fer shRNA–resistant construct, 5′-TATGGAAAGAAAGGAGAGACTGTCTAAATTTGAGTCTATTCGTC-3′ and 5′-GACGAATAGACTCAAATTTAGACAGTCTCTCCTTTCTTTCCATA-3′ and SHP-2 shRNA1–resistant constructs, 5′-GAGAGAGGGAAGAGTAAATGCGTCAAGTACTGGCC-3′ and 5′-GGCCAGTACTTGACGCATTTACTCTTCCCTCTCC-3′.

Primary neuronal culture, gene transfer, and peptide treatment

Dissociated hippocampal neurons were prepared from embryonic day 18 Sprague-Dawley rats as described previously (Bamji et al., 2003) using procedures approved by the University of California, San Francisco committee on animal research. Cells were plated at 75,000 cells/ml (192 cells/mm^2) on 18-mm coverslips coated with poly-L-lysine in 12-well plates. For imaging analyses, neurons were transfected at 10 DIV using Lipofectamine 2000 (Invitrogen). To get high transfection efficiency for immunoblotting, trans-synaptic dendritic spine analysis, and electrophysiology, neurons were electroporated with nucleofactor (Amaxa Biosystems) before plating according to the manufacturer's instructions. FerP and FerCo were applied directly into the maintenance medium at 5 μg/ml of final concentration. For lentiviral expression, viral particles were packaged in 293T cells and applied to the neurons at 7 DIV (multiplicity of infection 10).

Immunoprecipitation (IP) and immunoblotting

14 DIV hippocampal neurons were lyzed in denaturing IP buffer (1% SDS, 50 mM Hepes, pH 7.4, 150 mM NaCl, 1 mM sodium vanadate, 10 mM sodium fluoride, and 1 tablet/10 ml Complete Mini), boiled, and five times diluted with IP buffer without SDS. Lysates were clarified by centrifugation, and protein concentrations were determined using bicinchoninic acid reagent (Thermo Fisher Scientific). Aliquots of clarified lysates containing 1.5 mg of total protein were incubated with 3 μg of anti–β-catenin for 5 h followed by an additional incubation with Dynabead protein G (Invitrogen) for 1 h. The immunoprecipitates were washed three times with IP buffer. After SDS sample buffer (100 mM Tris, pH 6.8, 2% SDS, 10% glycerol, 5% β-mercaptoethanol, and 0.25% bromophenol blue) was added, samples were fractionated by SDS-PAGE and analyzed by immunoblotting.

Electrophysiology

In hippocampal cultures, fluorescent GFP signal was used to identify transfected cells (either Fer shRNA or control) from nontransfected WT neurons. Transfected and nontransfected neurons were paired for dual whole cell patch recording experiments by using an amplifier (MultiClamp 700B; MDS Analytical Technologies) and a converter (Digitdata 1322A; MDS Analytical Technologies) in conjunction with pClamp acquisition software (version 9.2; MDS Analytical Technologies). Paired cells were held at −70 mV. Individual stimuli (200 mV for 1 ms) were delivered to presynaptic neurons every 10 s, and eEPSCs at postsynaptic cells were sampled at 20 kHz. Pipette solution contained 120 mM K-gluconate, 10 mM KCl, 10 mM EGTA, and 10 mM Hepes buffered at pH 7.3. Bath solution consisted of 120 mM NaCl, 5 mM KCl, 3 mM $CaCl_2$, 2 mM $MgCl_2$, and 10 mM Hepes plus 20 µM bicuculline (Tocris Bioscience) to block inhibitory inputs.

Fluorescent imaging

9-wk-old mice were fixed with 4% paraformaldehyde, and 50-µm coronal sections were used for immunostaining. Cultured hippocampal neurons were fixed in 4% paraformaldehyde for 10 min, permeabilized with 0.1% Triton X-100 for 10 min, and blocked with 10% goat serum in PBS followed by primary antibody incubation at room temperature for 1 h. Cells were incubated with fluorescence-conjugated secondary antibodies. For FM4-64 loading, cells were incubated with 10 µm FM4-64 in high KCl-containing Tyrode buffer (67 mM NaCl, 60 mM KCl, 2 mM $CaCl_2$, 1 mM $MgCl_2$, 10 mM Hepes, pH 7.3, and 5 mM D-glucose) for 1 min and washed with regular Tyrode buffer (124 mM NaCl, 3 mM KCl, 2 mM $CaCl_2$, 1 mM $MgCl_2$, 10 M Hepes, pH 7.3, and 5 mM D-glucose). Unbound FM dye was further removed by incubation with 500 µm Advasep-7 in Tyrode buffer followed by two more washings with Tyrode. All buffers used after FM4-64 incubation contained 10 µM CNQX (6-cyano-7-nitroquinoxaline-2,3-dione) and 50 µM AP-5.

Fluorescence imaging was performed with a Pascal microscope (LSM5; Carl Zeiss, Inc.) equipped with a 63× 1.4 NA Plan Apochromat objective lens and Pascal software (Carl Zeiss, Inc.) or a microscope (Axiovert 200M; Carl Zeiss, Inc.) equipped with a 40× 1.3 oil/differential interference contrast Plan NeoFluor objective lens and Slidebook4.2 software (Intelligent Imaging Innovations, Inc.). For live cell imaging, neurons were maintained in a humidified chamber with 5% CO_2 and 37°C during the imaging.

Image processing and statistical analysis

Images were analyzed with Pascal or the ImageJ (National Institutes of Health) program and plug-in from the ImageJ website, and Excel (Microsoft) was used for statistical analyses.

First, to quantify the coverage of the puncta along the axons, the major axis lengths (feret) of individual puncta were measured at threshold 50 (for synaptophysin-GFP) or 40 (for synaptophysin-mOrange and GFP–Bsn-95-3938) with the analyze particle menu. Particles <5 pixels or >300 pixels were excluded from the analysis (1 pixel = 0.14 × 0.14 μm^2). Second, the lengths of axons were measured by the measure and label plug-in. Third, the sum of the ferets of individual puncta per 10 µm was calculated (sum of feret/axon length × 10) from each image field. Fourth, all values from the third step were normalized to control condition values in each experiment. The feret of each puncta was also used to obtain the cumulative percentage curve.

To quantify the mobility of presynaptic clusters, the velocity of synaptophysin-GFP puncta >0.5 μm^2 were obtained by the manual tracking plug-in of ImageJ. Kymograph was produced by the kymograph plug-in.

To examine the effect of presynaptic knockdown of Fer on apposed postsynaptic dendritic spine formation, two or three dendritic segments ∼50 µm in length and ∼50 µm away from the cell body were randomly picked from each mOrange-positive neuron. The contacts/crossings between GFP-labeled axons and mOrange-labeled dendrites were marked by the RG2B colocalization plug-in and counted manually. The density of the mOrange-labeled dendritic spine was counted without seeing GFP channel. Considering that the culture is a 1:1 mixture of GFP- and mOrange-expressing neurons and the density of contacts/crossings of GFP axons and mOrange dendrites were not significantly different between vector and Fer shRNA–transfected neurons (Fig. 3 F), we reason that ∼50% of axodendritic contacts are formed between GFP-labeled axons and mOrange-labeled dendrites within mOrange-positive dendrites.

For single puncta analysis (for vGlut1-pHluorin and synaptophysin-mOrange), the fluorescence intensity of every 0.01 µm along the major axis of each puncta was obtained from the Pascal program and imported to Excel. The center of the puncta was determined by finding the starting and ending points of the signals and was set as 0 along the x axis (distance). The intensity value (y axis) of each puncta was aligned along the distance, and all of the intensity values of every puncta at every 0.01 µm were averaged and plotted.

For colocalization analyses with PSD-95 and synaptophysin-GFP or FM4-64 and synaptophysin-GFP, the RG2B colocalization plug-in was used to obtain the second images of colocalized particles, and the coverage of second image particles were obtained by the aforementioned method. The coverage from the second images was divided by the coverage of synaptophysin-GFP from the same image.

To quantify the colocalization of endogenous Fer and vGlut1, the just another colocalization plug-in was used, and Pearson's coefficient was obtained from both correct and mismatched images (Pinches and Cline, 1998; Bolte and Cordelieres, 2006). At least 5,000 µm of axons from three different cultures was examined per each condition, and a Student's *t* test was performed.

Online supplemental material

Fig. S1 shows expression of Fer in hippocampal synapses, and Fig. S2 shows the verification of Fer shRNA. Fig. S3 shows the effect of kinase inhibition of Fer on excitatory synapse formation, and Fig. S4 schematizes the experiment to analyze the trans-synaptic effect of presynaptic Fer knockdown. Fig. S5 shows the verification of SHP-2 and PTP1B shRNAs. Videos 1–5 exhibit the presynaptic cluster dynamics. Videos 1–3 are videos of Fig. 2, and Videos 4 and 5 are videos from Fig. 6 (G and H). Online supplemental material is available at http://www.jcb.org/cgi/content/full/jcb.200807188/DC1.

We are grateful to P. Greer, D. Colman, M. Wheelock, T. Nakata, C. Garner, R.H. Edwards, R.Y. Tsien, S. Okabe, C. Lois, and I.M. Verma for providing essential reagents. We thank J. Arikkath for discussions and technical help, Y. Pan for technical help, and all other Reichardt laboratory members for discussion and/or help. We also thank Y. Cao and S. Junti for advice.

This work is supported by grants from the National Institutes of Health (P01 NS 16033) and the Simons Foundation to L.F. Reichardt; the Simons Foundation, Research to Prevent Blindness Young Investigator Award, and a National Institutes of Health grant (R21MH083090) to E.M. Ullian; a Knights Templar award to I.-F. Peng; a National Institutes of Health grant (R01 CA100467) to P.Z. Anastasiadis; and an L.L. Hillblom Foundation Fellowship (2006/2V) to S.-H. Lee.

Submitted: 31 July 2008
Accepted: 31 October 2008

References

Ahmari, S.E., J. Buchanan, and S.J. Smith. 2000. Assembly of presynaptic active zones from cytoplasmic transport packets. *Nat. Neurosci.* 3:445–451.

Alvarez, V.A., and B.L. Sabatini. 2007. Anatomical and physiological plasticity of dendritic spines. *Annu. Rev. Neurosci.* 30:79–97.

Anastasiadis, P.Z. 2007. p120-ctn: a nexus for contextual signaling via Rho GTPases. *Biochim. Biophys. Acta.* 1773:34–46.

Antonova, I., O. Arancio, A.C. Trillat, H.G. Wang, L. Zablow, H. Udo, E.R. Kandel, and R.D. Hawkins. 2001. Rapid increase in clusters of presynaptic proteins at onset of long-lasting potentiation. *Science.* 294:1547–1550.

Bamji, S.X., K. Shimazu, N. Kimes, J. Huelsken, W. Birchmeier, B. Lu, and L.F. Reichardt. 2003. Role of beta-catenin in synaptic vesicle localization and presynaptic assembly. *Neuron.* 40:719–731.

Bamji, S.X., B. Rico, N. Kimes, and L.F. Reichardt. 2006. BDNF mobilizes synaptic vesicles and enhances synapse formation by disrupting cadherin–β-catenin interactions. *J. Cell Biol.* 174:289–299.

Bolte, S., and F.P. Cordelieres. 2006. A guided tour into subcellular colocalization analysis in light microscopy. *J. Microsc.* 224:213–232.

Bourne, J.N., and K.M. Harris. 2008. Balancing structure and function at hippocampal dendritic spines. *Annu. Rev. Neurosci.* 31:47–67.

Bresler, T., M. Shapira, T. Boeckers, T. Dresbach, M. Futter, C.C. Garner, K. Rosenblum, E.D. Gundelfinger, and N.E. Ziv. 2004. Postsynaptic density assembly is fundamentally different from presynaptic active zone assembly. *J. Neurosci.* 24:1507–1520.

Castano, J., G. Solanas, D. Casagolda, I. Raurell, P. Villagrasa, X.R. Bustelo, A. Garcia de Herreros, and M. Dunach. 2007. Specific phosphorylation of p120-catenin regulatory domain differently modulates its binding to RhoA. *Mol. Cell. Biol.* 27:1745–1757.

Cochilla, A.J., J.K. Angleson, and W.J. Betz. 1999. Monitoring secretory membrane with FM1-43 fluorescence. *Annu. Rev. Neurosci.* 22:1–10.

Dresbach, T., A. Hempelmann, C. Spilker, S. tom Dieck, W.D. Altrock, W. Zuschratter, C.C. Garner, and E.D. Gundelfinger. 2003. Functional regions of the presynaptic cytomatrix protein bassoon: significance for synaptic targeting and cytomatrix anchoring. *Mol. Cell. Neurosci.* 23:279–291.

Dresbach, T., V. Torres, N. Wittenmayer, W.D. Altrock, P. Zamorano, W. Zuschratter, R. Nawrotzki, N.E. Ziv, C.C. Garner, and E.D. Gundelfinger. 2006. Assembly of active zone precursor vesicles: obligatory trafficking of presynaptic cytomatrix proteins Bassoon and Piccolo via a trans-Golgi compartment. *J. Biol. Chem.* 281:6038–6047.

Dunah, A.W., E. Hueske, M. Wyszynski, C.C. Hoogenraad, J. Jaworski, D.T. Pak, A. Simonetta, G. Liu, and M. Sheng. 2005. LAR receptor protein tyrosine phosphatases in the development and maintenance of excitatory synapses. *Nat. Neurosci.* 8:458–467.

Elia, L.P., M. Yamamoto, K. Zang, and L.F. Reichardt. 2006. p120 catenin regulates dendritic spine and synapse development through Rho-family GTPases and cadherins. *Neuron.* 51:43–56.

Goda, Y., and G.W. Davis. 2003. Mechanisms of synapse assembly and disassembly. *Neuron.* 40:243–264.

Ha, C.H., A.M. Bennett, and Z.G. Jin. 2008. A novel role of vascular endothelial cadherin in modulating c-Src activation and downstream signaling of vascular endothelial growth factor. *J. Biol. Chem.* 283:7261–7270.

Huber, A.H., and W.I. Weis. 2001. The structure of the beta-catenin/E-cadherin complex and the molecular basis of diverse ligand recognition by beta-catenin. *Cell.* 105:391–402.

Kim, H.J., A.M. Han, J.H. Shim, H.H. Yoon, H. Kwon, and Y.K. Kwon. 2007. Shp2 is involved in neuronal differentiation of hippocampal precursor cells. *Arch. Pharm. Res.* 30:750–754.

Kogata, N., M. Masuda, Y. Kamioka, A. Yamagishi, A. Endo, M. Okada, and N. Mochizuki. 2003. Identification of Fer tyrosine kinase localized on microtubules as a platelet endothelial cell adhesion molecule-1 phosphorylating kinase in vascular endothelial cells. *Mol. Biol. Cell.* 14:3553–3564.

Krueger, S.R., A. Kolar, and R.M. Fitzsimonds. 2003. The presynaptic release apparatus is functional in the absence of dendritic contact and highly mobile within isolated axons. *Neuron.* 40:945–957.

Lardi-Studler, B., and J.M. Fritschy. 2007. Matching of pre- and postsynaptic specializations during synaptogenesis. *Neuroscientist.* 13:115–126.

Lilien, J., and J. Balsamo. 2005. The regulation of cadherin-mediated adhesion by tyrosine phosphorylation/dephosphorylation of beta-catenin. *Curr. Opin. Cell Biol.* 17:459–465.

Lim, B.K., N. Matsuda, and M.M. Poo. 2008. Ephrin-B reverse signaling promotes structural and functional synaptic maturation in vivo. *Nat. Neurosci.* 11:160–169.

McAllister, A.K. 2007. Dynamic aspects of CNS synapse formation. *Annu. Rev. Neurosci.* 30:425–450.

Mitchell, S.J., and T.A. Ryan. 2004. Syntaxin-1A is excluded from recycling synaptic vesicles at nerve terminals. *J. Neurosci.* 24:4884–4888.

Mohi, M.G., and B.G. Neel. 2007. The role of Shp2 (PTPN11) in cancer. *Curr. Opin. Genet. Dev.* 17:23–30.

Murase, S., E. Mosser, and E.M. Schuman. 2002. Depolarization drives beta-catenin into neuronal spines promoting changes in synaptic structure and function. *Neuron.* 35:91–105.

Nakata, T., S. Terada, and N. Hirokawa. 1998. Visualization of the dynamics of synaptic vesicle and plasma membrane proteins in living axons. *J. Cell Biol.* 140:659–674.

Okabe, S., A. Miwa, and H. Okado. 2001. Spine formation and correlated assembly of presynaptic and postsynaptic molecules. *J. Neurosci.* 21:6105–6114.

Okuda, T., L.M. Yu, L.A. Cingolani, R. Kemler, and Y. Goda. 2007. beta-Catenin regulates excitatory postsynaptic strength at hippocampal synapses. *Proc. Natl. Acad. Sci. USA.* 104:13479–13484.

Pao, L.I., K. Badour, K.A. Siminovitch, and B.G. Neel. 2007. Nonreceptor protein-tyrosine phosphatases in immune cell signaling. *Annu. Rev. Immunol.* 25:473–523.

Piedra, J., S. Miravet, J. Castano, H.G. Palmer, N. Heisterkamp, A. Garcia de Herreros, and M. Dunach. 2003. p120 Catenin-associated Fer and Fyn tyrosine kinases regulate beta-catenin Tyr-142 phosphorylation and beta-catenin-alpha-catenin interaction. *Mol. Cell. Biol.* 23:2287–2297.

Pinches, E.M., and H.T. Cline. 1998. Distribution of synaptic vesicle proteins within single retinotectal axons of *Xenopus* tadpoles. *J. Neurobiol.* 35:426–434.

Rhee, J., T. Buchan, L. Zukerberg, J. Lilien, and J. Balsamo. 2007. Cables links Robo-bound Abl kinase to N-cadherin-bound beta-catenin to mediate Slit-induced modulation of adhesion and transcription. *Nat. Cell Biol.* 9:883–892.

Roura, S., S. Miravet, J. Piedra, A. Garcia de Herreros, and M. Dunach. 1999. Regulation of E-cadherin/catenin association by tyrosine phosphorylation. *J. Biol. Chem.* 274:36734–36740.

Ryan, T.A., and H. Reuter. 2001. Measurements of vesicle recycling in central neurons. *News Physiol. Sci.* 16:10–14.

Saglietti, L., C. Dequidt, K. Kamieniarz, M.C. Rousset, P. Valnegri, O. Thoumine, F. Beretta, L. Fagni, D. Choquet, C. Sala, et al. 2007. Extracellular interactions between GluR2 and N-cadherin in spine regulation. *Neuron.* 54:461–477.

Sallee, J.L., E.S. Wittchen, and K. Burridge. 2006. Regulation of cell adhesion by protein-tyrosine phosphatases: II. Cell-cell adhesion. *J. Biol. Chem.* 281:16189–16192.

Sieburth, D., Q. Ch'ng, M. Dybbs, M. Tavazoie, S. Kennedy, D. Wang, D. Dupuy, J.F. Rual, D.E. Hill, M. Vidal, et al. 2005. Systematic analysis of genes required for synapse structure and function. *Nature.* 436:510–517.

Tada, T., and M. Sheng. 2006. Molecular mechanisms of dendritic spine morphogenesis. *Curr. Opin. Neurobiol.* 16:95–101.

Tai, C.Y., S.P. Mysore, C. Chiu, and E.M. Schuman. 2007. Activity-regulated N-cadherin endocytosis. *Neuron.* 54:771–785.

Togashi, H., K. Abe, A. Mizoguchi, K. Takaoka, O. Chisaka, and M. Takeichi. 2002. Cadherin regulates dendritic spine morphogenesis. *Neuron.* 35:77–89.

Ukropec, J.A., M.K. Hollinger, S.M. Salva, and M.J. Woolkalis. 2000. SHP2 association with VE-cadherin complexes in human endothelial cells is regulated by thrombin. *J. Biol. Chem.* 275:5983–5986.

Voglmaier, S.M., K. Kam, H. Yang, D.L. Fortin, Z. Hua, R.A. Nicoll, and R.H. Edwards. 2006. Distinct endocytic pathways control the rate and extent of synaptic vesicle protein recycling. *Neuron.* 51:71–84.

Xu, G., A.W. Craig, P. Greer, M. Miller, P.Z. Anastasiadis, J. Lilien, and J. Balsamo. 2004. Continuous association of cadherin with beta-catenin requires the non-receptor tyrosine-kinase Fer. *J. Cell Sci.* 117:3207–3219.

Xu, W., and D. Kimelman. 2007. Mechanistic insights from structural studies of beta-catenin and its binding partners. *J. Cell Sci.* 120:3337–3344.

Yamada, S., and W.J. Nelson. 2007. Synapses: sites of cell recognition, adhesion, and functional specification. *Annu. Rev. Biochem.* 76:267–294.

Yanagisawa, M., D. Huveldt, P. Kreinest, C.M. Lohse, J.C. Cheville, A.S. Parker, J.A. Copland, and P.Z. Anastasiadis. 2008. A p120 catenin isoform switch affects Rho activity, induces tumor cell invasion, and predicts metastatic disease. *J. Biol. Chem.* 283:18344–18354.

Zhang, B., S. Luo, X.P. Dong, X. Zhang, C. Liu, Z. Luo, W.C. Xiong, and L. Mei. 2007. Beta-catenin regulates acetylcholine receptor clustering in muscle cells through interaction with rapsyn. *J. Neurosci.* 27:3968–3973.